Redox regulation of CD21 shedding involves signaling via PKC and indicates the formation of a juxtamembrane stalk

Annette Aichem[1], Madhan Masilamani[2,*] and Harald Illges[1,2,‡,§]

[1]Biotechnology Institute Thurgau at the University of Konstanz, Konstanzer Str. 19, 8274 Tägerwilen, Switzerland
[2]University of Konstanz, Department of Biology, Faculty of Sciences, Universitätsstrasse 10, 78457 Konstanz, Germany
*Present address: Receptor Cell Biology Section, Laboratory of Allergic Diseases, National Institute of Allergy and Infectious Diseases, National Institutes of Health, Rockville, MD 20852, USA
‡Present address: University of Applied Sciences, Department of Natural Sciences, Immunology and Cell Biology, von-Liebig-Strasse 20, 53359 Rheinbach, Germany
§Author for correspondence (e-mail: Harald.Illges@fh-brs.de)

Accepted 20 March 2006
Journal of Cell Science 119, 2892-2902 Published by The Company of Biologists 2006
doi:10.1242/jcs.02984

Summary

Soluble CD21 (sCD21), released from the plasma membrane by proteolytic cleavage (shedding) of its extracellular domain (ectodomain) blocks B cell/follicular dendritic cell interaction and activates monocytes. We show here that both serine- and metalloproteases are involved in CD21 shedding. Using the oxidant pervanadate to mimic B cell receptor activation and thiol antioxidants such as *N*-acetylcysteine (NAC) and glutathione (GSH) we show that CD21 shedding is a redox-regulated process inducible by oxidation presumably through activation of a tyrosine kinase-mediated signal pathway involving protein kinase C (PKC), and by reducing agents that either directly activate the metalloprotease and/or modify intramolecular disulfide bridges within CD21 and thereby facilitate access to the cleavage site. Lack of short consensus repeat 16 (SCR16) abolishes CD21 shedding, and opening of the disulfide bridge between cys-2 (Cys941) and cys-4 (Cys968) of SCR16 is a prerequisite for CD21 shedding. Replacing these cysteines with selenocysteines (thereby changing the redox potential from –180 to –381 mV) results in a loss of inducible CD21 shedding, and removing this bridge by exchanging these cysteines with methionines increases CD21 shedding.

Key words: B cells, CD21, Complement receptor, Cell activation, Redox potential, Selenocysteine, Diselenide bridge

Introduction

CD21 (complement receptor type 2, CR2) is a 145 kDa type I transmembrane glycoprotein that was initially described as the receptor for fragments of complement component C3 on immune complexes and for the Epstein Barr virus (EBV) (Fingeroth et al., 1984; Weis et al., 1984). The protein consists of an extracellular part of 15 or 16 tandemly repeated short consensus repeats (SCRs), depending on the alternative splicing of exon 11, a 28 amino acid transmembrane portion and a 34 amino acid cytoplasmic tail (Moore et al., 1987; Weis et al., 1988). CD21 is expressed in mature B lymphocytes and B cell lines, but not on early pre and pro B cells and late developmental stages (Schwab and Illges, 2001; Tedder et al., 1984). In addition it is expressed in low amounts on subsets of thymocytes, T cells, human follicular dendritic cells (Delibrias et al., 1994; Fischer et al., 1991; Reynes et al., 1985), epithelial cells such as the 293 cell line (Fingeroth et al., 1999), astrocytes (Gasque et al., 1996) and basophilic cells (Bacon et al., 1993). CD21 is necessary for B cell activation to T cell-dependent antigens (Ahearn et al., 1996) and for the survival of B cells in the germinal center reaction (Fischer et al., 1998).

A variety of cell-surface proteins including L-selectin, TNFα receptor and the EGF receptor appear as soluble proteins after shedding their ectodomains from the plasma membrane (reviewed by Dello Sbarba and Rovida, 2002). The 126 kDa sCD21 is also generated by shedding of the CD21 ectodomain and is found in human plasma and in cell culture supernatants of human lymphoid cells (Huemer et al., 1993; Ling et al., 1991; Masilamani et al., 2002; Myones and Ross, 1987). As sCD21 binds to its ligands in plasma, activates monocytes through binding to cell surface CD23 (Fremeaux-Bacchi et al., 1998) and inhibits B cell/follicular dendritic cell interactions (Qin et al., 1998), the amount of sCD21 could be a modulator of immunity. Altered human plasma levels of sCD21 are correlated to rheumatoid arthritis, systemic lupus erythematosus (SLE), Sjögren's Syndrome and other diseases (Huemer et al., 1993; Ling et al., 1991; Lowe et al., 1989; Masilamani et al., 2004; Masilamani et al., 2003b).

The CD21 sheddase has not yet been identified but most of the known shedding proteases belong to metalloprotease families such as matrix-metalloproteases (MMP) and ADAMs (a disintegrin and metalloprotease). These proteases are often synthesized as inactive precursors and become activated through proteolytic cleavage of their pro-domain, e.g. by serine proteases (reviewed by Steiner et al., 1992). Metalloproteases generally cleave their substrate close to the plasma membrane, independent of a consensus sequence in a 'stalk' region with minimum length requirements, and dependent on the steric availability of the cleavage site (reviewed by Dello Sbarba and Rovida, 2002). Based on the apparent molecular mass of sCD21 and mass spectroscopy data of sCD21 we suggested that the cleavage site of CD21 is located within SCR16,

adjacent to the plasma membrane (Masilamani et al., 2002; Masilamani et al., 2003a).

The cellular redox status plays a crucial role in the regulation of many cellular processes. We recently showed that CD21 shedding in B cells is inducible by crosslinking the B cell receptor (BCR) and CD40 or by stimulating the cells with the mitogen phorbol 12-myristate 13-acetate (PMA) plus ionomycin (Masilamani et al., 2003a). The effect of oxidants such as pervanadate are connected to B cell activation because they induce a similar signal pathway as is induced by antigen stimulation (reviewed by Reth, 2002). Here, we investigated the effect of the oxidant pervanadate as well as the thiol antioxidants *N*-acetylcysteine (NAC), reduced L-glutathione (GSH) and β-mercaptoethanol (2-ME) on activation of CD21 shedding in B cells and the CD21 transfected epithelial cell line 293. Furthermore, several CD21 constructs were used to characterize the putative cleavage site within CD21. We further report about the development of a system that allows the efficient substitution of cysteine residues by selenocysteines, thereby generating CD21 proteins with a much lower redox potential than the native protein. By mutation of cysteines to methionine or selenocysteine we showed that the reduction of the disulfide bridge between cys-2 (Cys941) and cys-4 (Cys968) of SCR16 is a prerequisite for CD21 shedding.

Results

PMA/CaI-induced CD21 shedding in 293 cells

We have previously shown that activation of B cells with the mitogen PMA plus Ca^{2+} ionophore ionomycin (CaI) or by crosslinking the BCR together with CD40 induced CD21 shedding (Masilamani et al., 2003a). To gain additional information about the regulation of CD21 shedding in B cells as well as in non-lymphoid CD21-expressing cells, primary B cells, Daudi and Raji B cells and the epithelial cell line 293 were chosen. Because 293 cells express only low levels of endogenous CD21 (Fingeroth et al., 1999) we stably transfected the cells with the CD21 expression plasmid pSFFVneo-CR2-M1 (Carel et al., 1989) (293-CD21 cells). Confocal microscopy revealed that the exogenous CD21 is expressed and localized on the cell surface of the 293-CD21 cells (Fig. 1A). By flow cytometry we verified that these cells do not express additional B cell markers such as CD19 and CD20 (data not shown). Next we asked whether induction of CD21 shedding in 293-CD21 cells would be comparable to that of B cells. Therefore, we stimulated the cells with PMA, CaI or PMA plus CaI for 4 hours at 37°C. Cell lysates were prepared and subjected to western blot analysis. PMA alone did not significantly decrease CD21, but PMA in combination with CaI decreased CD21 in 293-CD21 cells to almost undetectable levels (Fig. 1B). The corresponding results were obtained by measuring sCD21 from the cell culture supernatants by ELISA. Whereas CaI alone already significantly increased the amount of sCD21 by a factor of 1.5, PMA/CaI led to an even stronger increase of sCD21 (2.3 times) as compared to the untreated control (Fig. 1C). These data showed that induction of CD21 shedding in 293-CD21 cells is similar to that of B cells.

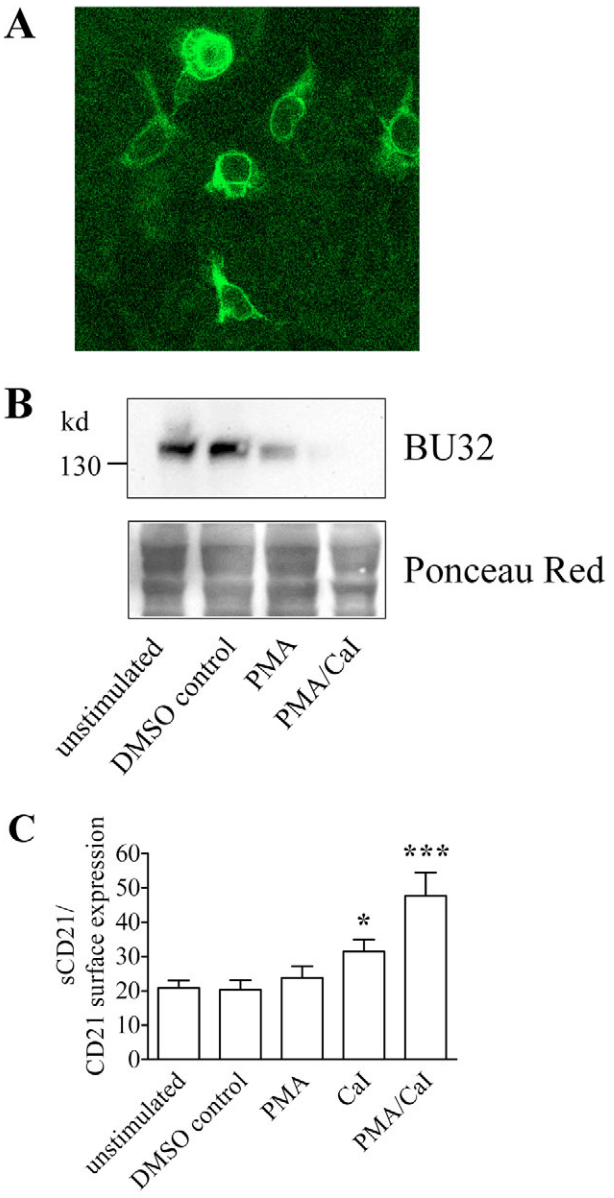

Fig. 1. PMA/CaI-induced CD21 shedding in 293-CD21 cells. (A) 293-CD21cells were stained with the monoclonal anti-CD21 FITC-labeled antibody BL13. Expression and cell surface localization of the exogenous CD21 was verified by confocal microscopy. (B) Western blot analysis of 293-CD21 cells after 4 hours of stimulation with 10 μM PMA, 10 μM PMA + 1 μM CaI or the solvent control DMSO. 30 μg of protein lysate per lane were subjected to western blot analysis using the monoclonal anti-CD21 antibody BU32 (upper panel). The blot was stained with Ponceau Red to control the amount of loaded protein (lower panel). (C) Determination of sCD21 (measured as pg sCD21/ml/median fluorescence intensity of 293-CD21 cells) in cell culture supernatants from 293-CD21 cells by ELISA. Cell culture supernatants were collected after incubation of the cells for 4 hours with 10 μM PMA, 1 μM CaI, 10 μM PMA + 1 μM CaI or the solvent control DMSO. Data are mean of five independent experiments each measured in triplicate.

The oxidant pervanadate induces CD21 shedding

Incubation of B cells with the oxidant pervanadate results in a tyrosine phosphorylation pattern similar to that observed after antigen stimulation (reviewed by Reth, 2002). Because B cell activation by crosslinking the BCR and CD40 induced CD21 shedding (Masilamani et al., 2003a), we were interested to know whether pervanadate also induces CD21 shedding. Daudi

B cells as well as peripheral blood mononuclear cells (PBMC) isolated from four healthy donors were incubated for 4 hours in serum-free medium with increasing concentrations of pervanadate. Incubation of Daudi B cells with 25 μM or 200 μM pervanadate resulted in a 1.4- or 1.7-fold significant increase of sCD21 in the cell culture supernatants, respectively, as measured by ELISA (Fig. 2A). Concomitantly, the cell surface CD21 of primary B cells was significantly decreased by 66% and 78% compared to the untreated control after incubation with 200 μM or 1 mM pervanadate, respectively (Fig. 2B). Thus, CD21 shedding from B cells can be induced very efficiently by the oxidant pervanadate.

Pervanadate activates B cells and leads to tyrosine phosphorylation of signal components downstream of the BCR (reviewed by Reth, 2002). Therefore, we were interested to know if pervanadate is also able to induce CD21 shedding in 293-CD21 cells, expressing CD21 but not the BCR or CD19. As shown in Fig. 2C, incubation of 293-CD21 cells with 25 μM, 200 μM or 1 mM pervanadate significantly augmented sCD21 in the cell culture supernatant by a factor of 1.4, 1.7 or 2.4, respectively, as compared to the untreated control. For all cell types and pervanadate concentrations tested, the corresponding decrease of cell surface CD21 was measured by flow cytometry with gating on living, CD21-positive cells (data not shown). We therefore concluded that pervanadate induces CD21 shedding independent of BCR and CD19 expression.

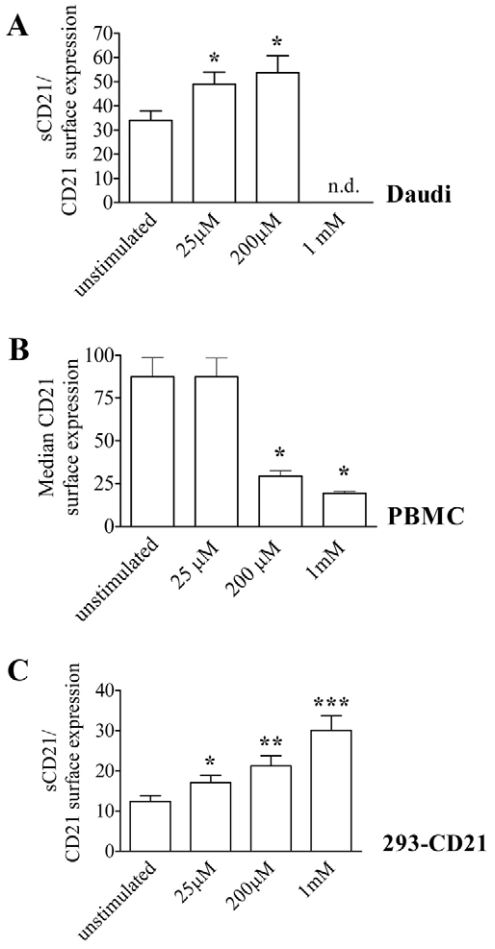

Fig. 2. Pervanadate induced CD21 shedding in Daudi B cells, PBMC and 293-CD21 cells. 2×10^6 Daudi B cells/ml (A), 3.4×10^6 PBMC/ml isolated from four healthy donors (B) and 293-CD21 cells (C) were incubated for 4 hours with increasing concentrations of pervanadate. (A,C) Cell culture supernatants from 293-CD21 and Daudi B cells were collected and the amount of sCD21 was determined by ELISA. Data for 293-CD21 cells are means of three independent experiments, data for Daudi B cells are means of four independent experiments, each measured in triplicate (pg sCD21/ml/median fluorescence intensity of respective cells. (B) PBMC from four healthy donors were collected and cell surface CD21 of primary B cells was measured by flow cytometry after staining with anti-CD21-RPE. n.d.: not determined.

CD21 shedding is induced by thiol antioxidants

Because pervanadate is an oxidizing agent, we were interested to know if reducing agents such as thiol antioxidants may regulate CD21 shedding as well. 293-CD21 cells, Daudi B cells and PBMC were incubated for 4 hours with the thiol

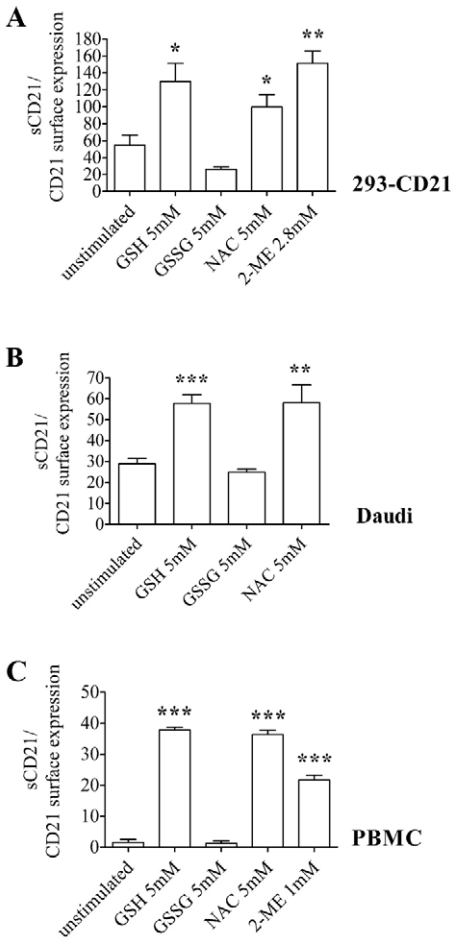

Fig. 3. Induction of CD21 shedding by thiol antioxidants. 293-CD21 cells (A), Daudi B cells (2×10^6 cells/ml) (B) and PBMC from four healthy donors (5×10^6 cells/ml) (C) were stimulated for 4 hours with 5 mM reduced glutathione (GSH), 5 mM oxidized glutathione (GSSG), 5 mM NAC, 1 mM or 2.8 mM β-mercaptoethanol (2-ME). Cell culture supernatants were collected and sCD21 was measured by ELISA; values expressed as pg sCD21/ml/median fluorescence intensity of respective cells. Data are means of three independent experiments each measured in triplicate.

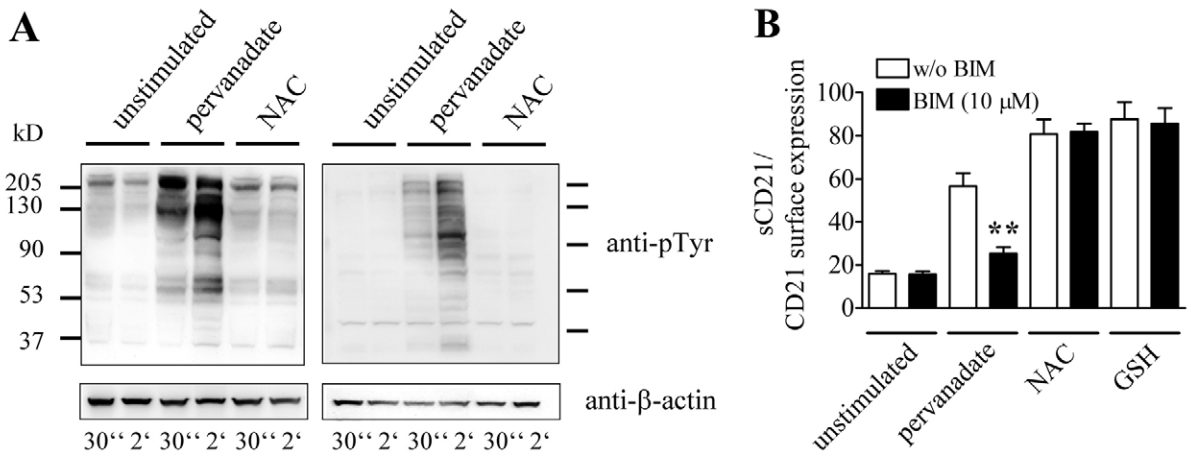

Fig. 4. Oxidants and thiol antioxidants operate at different sites of CD21 shedding induction. (A) Analysis of the tyrosine phosphorylation pattern after incubation of 293 cells stably transfected with construct B (293-CD21-B cells) (left panel) and Daudi B cells (right panel) with the CD21 shedding stimuli pervanadate (200 μM) or NAC (5 mM). Cells were stimulated for 30 seconds or 2 minutes at 37°C, lysed and subjected to western blot analysis (1.6×10^5 293-CD21-B cells/lane; 1.3×10^6 Daudi B cells/lane) using an anti-phosphotyrosine antibody. As loading control, both blots were stained with an anti-β-actin antibody (lower panel). (B) Pervanadate-, but not NAC- and GSH-induced CD21 shedding is inhibited by the PKC inhibitor BIM. 293-CD21-B cells were preincubated for 1 hour with or without 10 μM BIM and subsequently incubated for 4 hours with 1 mM pervanadate, 5 mM NAC or 5 mM GSH in the presence or absence of 10 μM BIM. Cell culture supernatants were collected and sCD21 was measured by ELISA (values expressed as pg sCD21/ml/median fluorescence intensity of 293-CD21-B cells). Data are means of three independent experiments each measured in triplicate.

antioxidants glutathione (GSH), *N*-acetylcysteine (NAC) and β-mercaptoethanol (2-ME) (Fig. 3). Whereas sCD21 increased significantly in cell culture supernatants of 293-CD21 and Daudi cells by a factor of two to three (Fig. 3A,B), sCD21 in supernatants of PBMC increased by 13 to 23 times as compared to the untreated control (Fig. 3C). The corresponding decrease of cell surface CD21 was measured by flow cytometry (data not shown). In all three cell types tested, oxidized glutathione (GSSG), possessing no reducing activity, had no effect and served as control.

Oxidants and thiol antioxidants operate at different sites of CD21 shedding induction

Since the oxidant pervanadate as well as all antioxidants tested activated shedding of CD21 we were interested to know if these opposed classes of substances interfere at different sites of the shedding induction pathway. We compared the tyrosine phosphorylation pattern of 293-CD21-B cells and Daudi B cells after incubation of the cells for 30 seconds or 2 minutes with or without pervanadate or NAC (Fig. 4A). In both cell types, incubation with pervanadate led to strong tyrosine phosphorylation, whereas incubation with NAC (Fig. 4A) or GSH (not shown) had no effect on the tyrosine phosphorylation level, even after a longer incubation time of 10 minutes (data not shown). We further investigated the effect of the protein kinase C inhibitor bisindolylmaleimide (BIM) on pervanadate, NAC and GSH induced CD21 shedding in 293-CD21-B cells by ELISA. As shown in Fig. 4B, only the pervanadate-induced CD21 shedding could be significantly inhibited by preincubation of the cells with BIM, but not the thiol-antioxidant-induced shedding. The same results were obtained for two independent 293 clones also transfected with CD21 construct B (data not shown). Based on these results we suggest that the oxidant pervanadate and the thiol antioxidants target different molecules involved in CD21 shedding.

Serine protease and metalloproteases are involved in CD21 shedding

To gain information about the putative families of proteases involved in CD21 shedding, we tested several metallo- and serine protease inhibitors. Several concentrations of the inhibitors were tested (data not shown) and effective concentrations of each inhibitor were chosen for further experiments.

Raji B cells were cultured for 24 hours in the presence of the metalloprotease inhibitors MMPi-I, -II, -III, EDTA or the serine protease inhibitor α1-antitrypsin (AAT). As measured by ELISA, AAT significantly reduced the amount of sCD21 in the cell culture supernatants (Fig. 5A). The same results were obtained with MMPi-I, -III and EDTA.

We further tested if the PMA/CaI-induced CD21 shedding can be inhibited by these protease inhibitors. For this, PBMC from three healthy donors were incubated for 4 hours with AAT, PMA or AAT+PMA, and sCD21 in the cell culture supernatant was measured by ELISA. Incubation with AAT alone already reduced the amount of spontaneously released sCD21 from PBMC significantly by about 80%. In addition, PMA-induced CD21 shedding was also significantly decreased in the presence of AAT (Fig. 5B). As shown in Fig. 5C, PMA/CaI-induced CD21 shedding in 293-CD21 cells could be significantly reduced by tissue inhibitor of metalloprotease-II (TIMP-II) and MMPi-I. The serine protease inhibitor AAT also significantly inhibited the PMA/CaI-induced shedding in these cells. These data suggest, that serine- as well as the metalloproteases are involved in shedding of CD21.

We further tested whether NAC-induced CD21 shedding could be inhibited by the same protease inhibitors acting on PMA/CaI-induced CD21 shedding. Two CD21-expressing 293-CD21-B clones were stimulated with 5 mM NAC in the presence or absence of MMPi-I, -II -III or AAT, and sCD21

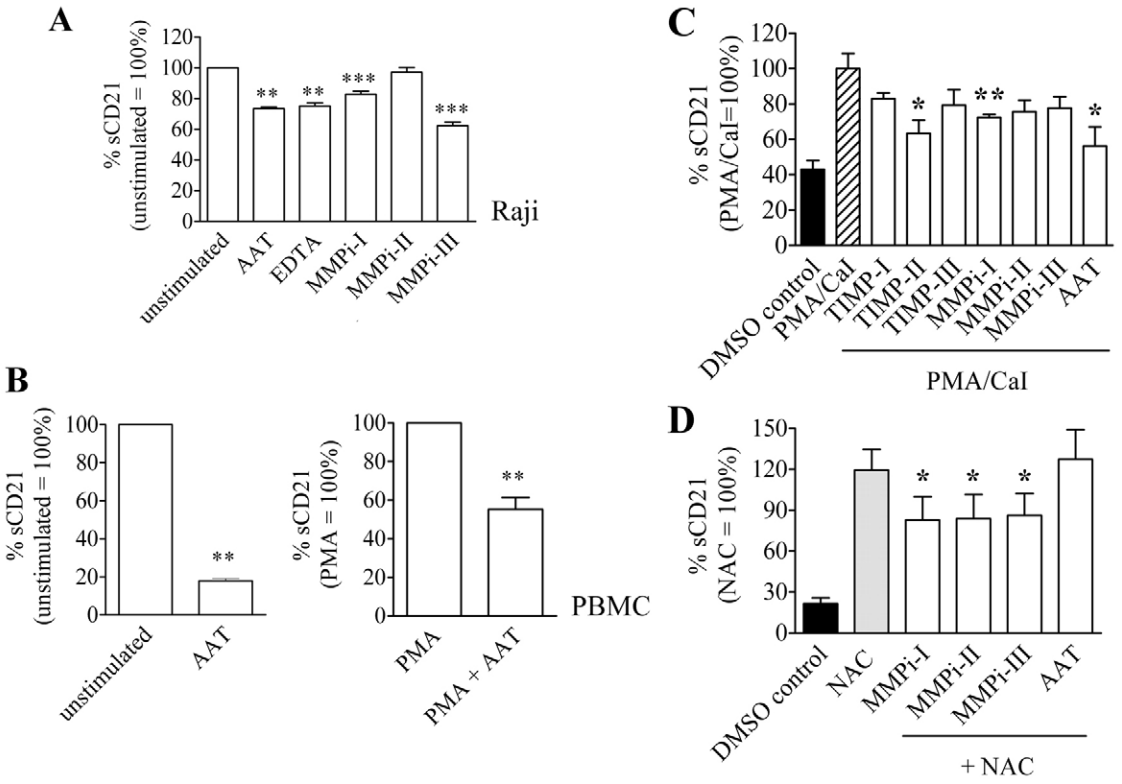

Fig. 5. CD21 shedding is inhibited by metallo- and serine protease inhibitors. (A) 5×10^6 Raji cells/ml were cultured for 24 hours in the presence of 200 μM MMPi-I, 50 nM MMPi-II, 200 nM MMPi-III, 1 mg/ml AAT or 2 μM EDTA. Cell culture supernatants were collected and sCD21 was measured by ELISA. (B) 5×10^6 PBMC/ml from three healthy donors were stimulated for 4 hours with 1 mg/ml AAT, 10 μM PMA or 1 mg/ml AAT and 10 μM PMA. Cell culture supernatants were collected and the amount of sCD21 was measured by ELISA. (C) 293-CD21 cells were preincubated in serum free IMDM for 1 hour at 37°C with TIMP-I (40 nM), TIMP-II (40 nM), TIMP-III (20 nM), MMPi-I (200 μM), MMPi-II (50 nM), MMPi-III (200 nM) or AAT (1 mg/ml) and subsequently stimulated for 4 hours with 10 μM PMA + 1 μM CaI in the presence of the inhibitors. Cell culture supernatants were collected and the amount of sCD21 was measured by ELISA. Data are means of three independent experiments each measured in triplicate. (D) Two 293-CD21-B clones (see Fig. 6 for description) were incubated for 1 hour at 37°C with MMPi-I (200 μM), MMPi-II (50 nM), MMPi-III (200 nM) or 1 mg/ml AAT and subsequently stimulated for 4 hours with 5 mM NAC in presence of the inhibitors. Cell culture supernatants were collected and the amount of sCD21 was measured by ELISA.

was measured by ELISA. NAC-induced shedding was significantly inhibited by all metalloprotease inhibitors tested (Fig. 5D). Although the serine protease inhibitor AAT significantly inhibited PMA/CaI-induced shedding, AAT did not inhibit NAC-induced shedding. Therefore, we suggest that NAC directly acts on a metalloprotease and not on signaling components involved in the CD21 shedding cascade.

CD21 shedding depends on SCR16

The SCRs of CD21 can be grouped into four homologous groups with the exception of SCR16 that does not belong to any of these groups. Each SCR contains four highly conserved cysteine residues forming two disulfide bridges between cys-1 and cys-3 and between cys-2 and cys-4 (Weis et al., 1988). We previously showed, by mass-spectrometry, that sCD21 consists of the extracellular portion of CD21 and suggested that the cleavage site is located directly adjacent to the plasma membrane (Masilamani et al., 2002; Masilamani et al., 2003a). This protein portion consists of SCR16 encoded by exon 16 of the CD21 *CR2* gene, with cys-1 (Cys912) forming a bridge with cys-3 (Cys955) and cys-2 (Cys941) with cys-4 (Cys968). We were interested to know whether cleavage of CD21 is sequence dependent, or if cleavage occurs sequence independently but at a position with a defined distance from the plasma membrane. We constructed a CD21 expression plasmid where we replaced exon 16 by exon 15, thereby deleting the putative cleavage site (Fig. 6A, construct A). As a control, the complete CD21 cDNA was cloned into the same plasmid (construct B). The constructs were stably transfected into 293 cells, and CD21 expression and surface localization was verified by flow cytometry (Fig. 6B). After induction of CD21 shedding with either PMA/CaI, pervanadate, NAC or GSH the amount of sCD21 was determined by ELISA. Cells expressing CD21 proteins lacking SCR16 (293-CD21-A cells, median fluorescence intensity: 1843) did not shed CD21, whereas cells transfected with the expression plasmid containing the complete CD21 cDNA (293-CD21-B cells, median fluorescence intensity: 2267) shed CD21 in very high amounts (Fig. 6C).

To exclude the possibility that the insertion of a *Bgl*II site during the construction of the CD21 expression vectors induced conformational changes resulting in inhibition of CD21 shedding, we designed three additional constructs (Fig. 6A) containing the complete CD21 cDNA but with *Bgl*II sites 3′ to exon 16 (construct C), 5′ to exon 16 (construct D), or with *Bgl*II sites flanking exon 16 (construct E). The constructs

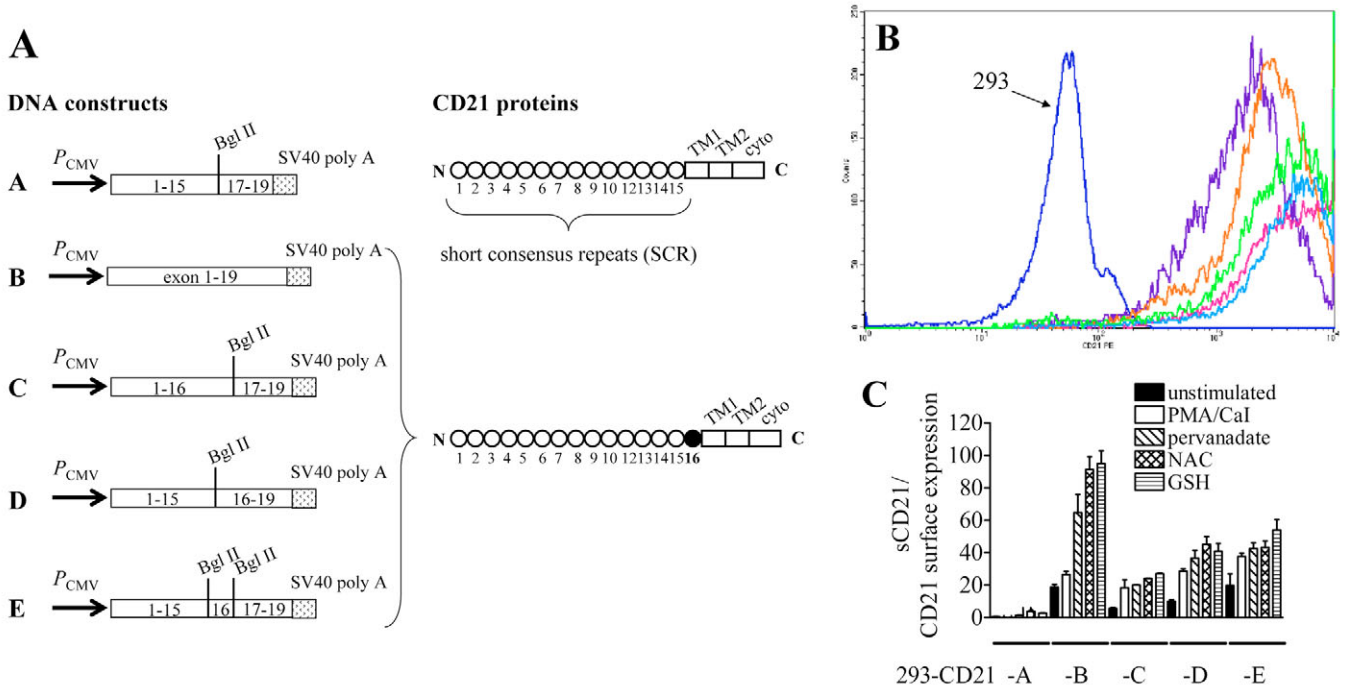

Fig. 6. SCR 16 is required for CD21 shedding. (A) Schematic presentation of CD21 constructs. Several CD21 cDNAs containing exon 16 (B-E) and one without (A) were cloned into the eucaryotic expression plasmid pEGFP-C1 as described in Materials and Methods. The resulting CD21 proteins are schematically shown on the right. (B) Verification of the expression and cell surface localization of the different CD21 mutant proteins expressed by 293 cells, stable transfected with the constructs shown in Fig. 6A. Cells were stained with anti-CD21-RPE and subjected to flow cytometry analysis. One clone of each cell line is shown (293-CD21-A, violet; -B, orange; -C, magenta; -D, light blue; -E, green). Untransfected 293 cells (blue) were stained as a control. (C) Determination of the amount of sCD21 in cell culture supernatants after stimulation of the cells for 4 hours at 37°C with 10 μM PMA + 1 μM CaI, 200 μM pervanadate, 5 mM NAC or 5 mM GSH. Cell culture supernatants were collected and sCD21 was measured by ELISA (values expressed as pg sCD21/ml/median fluorescence intensity of respective clones). Three clones of each construct were tested and gave the same results. Data are means of two independent experiments of a single clone of each cell line.

were transfected into 293 cells and CD21 expression and surface localization was verified by flow cytometry (Fig. 6B). All cell lines expressed significant amounts of cell surface CD21 (median fluorescence intensities of the clones shown in Fig. 6B,C: 293-CD21-C cells, 4826; -D cells, 4783; -E cells, 4293). As shown in Fig. 6C, shedding of CD21 proteins derived from these constructs could clearly be induced in comparison to CD21 proteins lacking SCR16 (CD21-A cells) although the amount of shed CD21 was decreased as compared to the control CD21 proteins encoded by construct B. Thus the inserted *Bgl*II site did not inhibit CD21 shedding in case of CD21 proteins lacking SCR16. Therefore, we conclude that CD21 shedding requires SCR16 and that shedding is reduced to background levels when this portion is removed from the protein.

Reduction of the disulfide bridge between cys-2 and cys-4 of SCR16 is a prerequisite for CD21 shedding

Substrates of metalloproteases are described to contain a juxtamembrane stalk with minimum length requirements and steric availability in order to allow access of the sheddase (reviewed by Dello Sbarba and Rovida, 2002). Oxidized CD21 contains only two amino acids between cys-4 of SCR16 and the plasma membrane, and therefore does not possess a juxtamembrane stalk that is comparable to the stalks of the metalloprotease substrates described so far. A reduction of the disulfide bridge between cys-2 and cys-4 of SCR16 would generate a stalk of 14 amino acids in length. Based on these findings we hypothesized that CD21 has to be at least partially reduced in order to generate a stalk allowing access of the sheddase. To prove this, we developed a system to efficiently exchange cysteines for selenocysteines (Sec). A diselenide bridge (Sec-Sec) has a much lower redox potential than a disulfide bridge [Cys-Cys: –180 mV (Siedler et al., 1993), Sec-Sec: –381 mV (Besse et al., 1997; Besse and Moroder, 1997)] and thus exists in the oxidized form under conditions where the disulfide bridges are already reduced. Therefore we were interested to know if shedding of the Sec-containing CD21 (CD21-Sec) would be abolished due to the inability to generate a stalk by opening the cysteine bridge between cys-2 and cys-4. By site-directed mutagenesis, the cysteine codons of cys-2 and cys-4 within SCR16 of construct CD21-E were changed to TGA (construct F, Fig. 7A). In the presence of a specific hairpin structure in the 3′ untranslated region (3′UTR) of the mRNA, the so called selenocysteine insertion sequence (SECIS), as well as specific SECIS-binding proteins, the Sec-specific elongation factor (eEFSec) and the Sec-tRNA^{Sec}, UGA is recognized as a UGA-Sec codon rather than as a stop codon (reviewed by Krol, 2002). As SECIS we inserted the 3′UTR of the selenium-dependent glutathione peroxidase PHGPx into the 3′UTR of the CD21 expression construct E. This SECIS element was chosen because it is reported to exhibit a high Sec

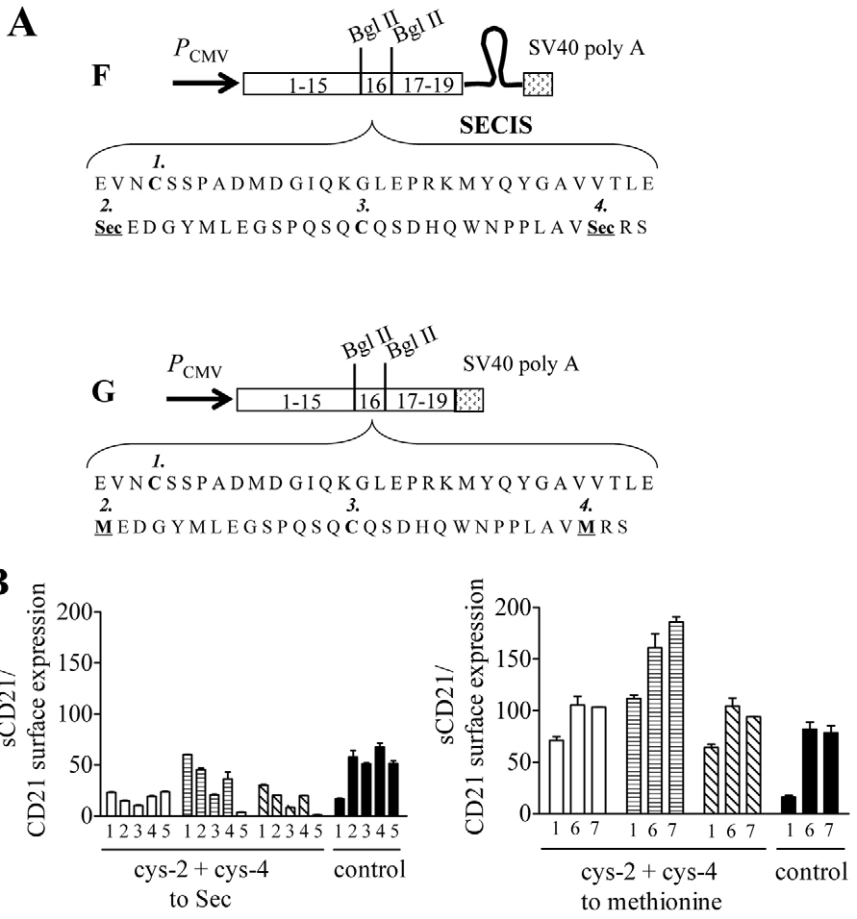

Fig. 7. Replacing the disulfide bridge between cys-2 and cys-4 of SCR16 by a diselenide bridge inhibits CD21 shedding. (A) Schematic presentation of CD21 constructs and the deduced amino acid sequence of SCR16 including the mutated cysteine residues. For the incorporation of selenocysteines instead of cysteines, the codons for cys-2 (Cys941) and cys-4 (Cys968) were exchanged for TGA by site-directed mutagenesis and the SECIS element of the selenium-dependent glutathione peroxidase PHGPx was cloned 3′ to exon 19 (construct F). In order to obtain a constitutively open bridge between cys-2 and cys-4, the same codons were replaced by methionine (construct G). (B) Determination of the amount of sCD21 in cell culture supernatants of three 293 clones stable transfected with the construct F (left panel) or G (right panel). Control cells were 293 cells stable transfected with construct B (Fig. 6A). Cells were incubated for 4 hours at 37°C (bars labeled 1, t_4 control) or stimulated for 4 hours at 37°C with 10 mM GSH (bars 2), 30 mM GSH (bars 3), 10 mM NAC (bars 4), 30 mM NAC (bars 5), 5 mM GSH (bars 6) or 5 mM NAC (bars 7). Cell culture supernatants were collected and sCD21 was measured by ELISA (values expressed as pg sCD21/ml/median fluorescence intensity of respective clones). Three clones of each cell line were tested in two independent experiments. Data are means of each single clone measured in triplicate.

incorporation efficiency than the SECIS elements of other glutathione peroxidases (Muller et al., 2003). In order to generate a CD21 protein with a constitutively open bridge between cys-2 and cys-4, the same cysteines were mutated to methionine (CD21-Met) (construct G, Fig. 7A). The constructs were transfected into 293 cells, growing in medium supplemented with 150 nM sodium selenite in case of the CD21-Sec-expressing cells, and the expression and surface localization of the mutated proteins was confirmed by immunoprecipitation (data not shown) and FACS analysis (median fluorescence intensity of the CD21-Sec clones shown in Fig. 7B: 710, 670 and 820 and of the CD21-Met clones: 1055, 850 and 813, respectively). Stimulation of the CD21-Sec-expressing cells with 5 mM NAC or GSH did not result in an increase in sCD21 in the cell culture supernatant (data not shown), presumably due to the much lower redox potential of CD21-Sec. In addition, even higher concentrations of both substances (10 or 30 mM) did not induce CD21 shedding, whereas in the control cells expressing wild-type CD21, CD21 shedding could clearly be induced (Fig. 7B, left panel). The same results were obtained when the cells were stimulated with 10 mM 2-ME, a strong reducing agent (data not shown). In contrast to this, 5 mM NAC or GSH induced CD21 shedding from CD21-Met-expressing cells even more strongly than in control cells (Fig. 7B, right panel). These results suggest that opening of the disulfide bridge between cys-2 and cys-4 of SCR16 is a necessary event during the process of induced CD21 shedding.

Discussion

The cellular redox status is a critical factor in signal transduction and gene expression. Many receptors start to signal in a ligand-independent manner after exposure to the strong oxidant pervanadate. Incubation of B cells with pervanadate results in a tyrosine phosphorylation pattern similar to that induced by BCR crosslinking by antigen (reviewed by Reth, 2002; Schieven et al., 1993; Uckun et al., 1992). We show here that pervanadate activates CD21 shedding in Daudi and primary B cells and in 293-CD21 epithelial cells. In addition we could inhibit pervanadate-induced CD21 shedding with the protein kinase C (PKC) inhibitor BIM. Thus, our data provide evidence that a tyrosine kinase-mediated signal transduction pathway involving PKC activation regulates CD21 shedding and that induction of CD21 shedding is not restricted to lymphoid cells. This supports previous experiments where we induced CD21 shedding by BCR/CD40 crosslinking and by PMA/CaI stimulation (Masilamani et al., 2003a). Recent reports have shown that shedding of several other proteins such as pro-EGF (Le Gall et al., 2003), the transferrin receptor (Kaup et al., 2002) or betaglycan (Velasco-Loyden et al., 2004) are also activated by pervanadate.

Since the oxidant pervanadate was very effective in activation of CD21 shedding we were interested in the effect of thiol antioxidants. NAC acts as scavenger of free radicals and serves as a precursor of GSH because it easily penetrates the cell where it is deacetylated to form L-cysteine, supporting

the biosynthesis of GSH. In addition it is a strong reducing agent that reduces disulfide bonds and therefore can directly modify the activity of several proteins (for a review, see De Vries and De Flora, 1993). Nishinaka and co-workers (Nishinaka et al., 2001) measured cell surface CD21 on B cells after incubation of the cells with increasing concentrations of NAC and suggested that NAC suppresses CD21 surface expression and that this is not due to CD21 shedding. In contrast to this we show that NAC, GSH or 2-ME induced CD21 shedding from B- as well as from 293-CD21 cells.

Using several protease inhibitors, we suggest that serine proteases as well as metalloproteases might be involved in spontaneous as well as PMA/CaI-induced shedding of CD21. None of the tested protease inhibitors led to a complete block of CD21 shedding. Therefore we have only information about the families of proteases involved in CD21 shedding and prefer to directly apply molecular biological tools to define the proteases involved. Many proteases are converted from an inactive pro-enzyme into an active form via a proteolytic process. Certain classes of metalloproteases such as members of the ADAM family are converted in the trans-Golgi compartment into their active form by furin-type serine endoproteases (Steiner et al., 1992). Therefore, our finding of two different classes of proteases involved in CD21 shedding suggests that the CD21 sheddase could exist in a pro-enzyme form as well. NAC-induced CD21 shedding in 293-CD21 cells was also significantly inhibited by the metalloprotease inhibitors MMPi-I, -II and -III but not by the serine protease inhibitor AAT that was effective in inhibiting PMA/CaI-induced CD21 shedding. Therefore, our data provide the first evidence that thiol antioxidants such as NAC can activate directly the metalloprotease involved in CD21 shedding. This is of particular interest because recent publications showed that metalloproteases are activated by oxidation and inhibited by reducing agents. Thus the CD21 sheddase might be the first example of a protease activated by reduction. Metalloproteases share a highly conserved domain in the pro-domain, bearing a cysteine residue that interacts with the zinc atom in the active center and therefore keeps the metalloprotease inactive. Dissociation of the cysteine residue, e.g. by oxidation, results in activation of the enzyme [the so called cysteine switch mechanism (reviewed by Van Wart and Birkedal-Hansen, 1990; Zucker et al., 2003)]. The same mechanism of activation is also described for TACE-mediated ectodomain shedding of cell surface proteins such as TNFα and the p75TNF receptor (Arribas and Merlos-Suárez, 2003). Inhibition of metalloprotease activities, in particularly MMP-2 and -9, by reducing agents has been reported. Buhimschi and co-workers (Buhimschi et al., 2000) and Uemura and co-workers (Uemura et al., 2001) showed that MMP-2 and -9 activities were inhibited after incubation with NAC.

In contrast to pervanadate, NAC did not induce tyrosine phosphorylation in 293-CD21-B and Daudi B cells. In addition we showed by ELISA, that the pervanadate-induced CD21 shedding could be significantly inhibited by the PKC inhibitor BIM, whereas NAC- and GSH-induced shedding was not affected. These results further confirm that the different shedding stimuli, such as PMA/CaI and pervanadate or the thiol antioxidants tested, target different sites of the shedding activation cascade. We propose that one part of the shedding pathway is stimulated by oxidation and involves the PKC, and that a reducing process can activate the metalloprotease. Since there is also a serine protease involved in CD21 shedding activation it is also possible that there are two different ways to activate the metalloprotease, one by reduction and the other one by activation through a serine protease.

Based on our previous data (Masilamani et al., 2002; Masilamani et al., 2003a) we suggest, that the proteolytic cleavage site of CD21 is localized directly adjacent to the plasma membrane. This protein portion consists of short consensus repeat 16 (SCR16) that is encoded by exon 16 of the *CR2* gene (Fujisaku et al., 1989). We show here that shedding of CD21 proteins lacking SCR16 was reduced to background levels. CD21 is a rod-shaped molecule and the single SCRs are believed to form globular structures. Each SCR contains four highly conserved cysteine residues that are disulfide bonded in a cys-1 to cys-3 and cys-2 to cys-4 pattern, forming a triple loop structure (Janatova et al., 1989). In the case of SCR16, Cys912 (cys-1) forms a bridge with Cys955 (cys-3) and Cys941 (cys-2) with Cys968 (cys-4). Based on the amino acid sequence, the SCRs of CD21 are grouped into four homologous groups with the exception of the juxtamembrane SCR16 that does not belong to any of these groups (Weis et al., 1988). This difference in homology concerning SCR16 could explain why SCR15 could not replace the function of SCR16 in CD21 shedding. However, we formally cannot exclude that the lack of SCR16 renders the structure of SCR15 inaccessible for the protease. Moreover, the inter-SCR linkers between the single SCRs differ in length and are built up of only three to eight amino acids (reviewed by Perkins et al., 2002). Oxidized CD21 contains only two amino acids between cys-4 of SCR16 and the plasma membrane, and only four amino acids from cys-1 of SCR16 to the most C-terminal cysteine (Cys907) of SCR15. Therefore, oxidized CD21 does not contain a juxtamembrane stalk that is comparable to the stalks of the metalloprotease substrates described so far. Proteases of the ADAM family such as TACE (ADAM 17) cleave their substrates dependent on specific structural requirements such as an unfolded stalk region with a minimum length of about 11 amino acids surrounding the cleavage site (Althoff et al., 2001; Arribas et al., 1997; Dello Sbarba and Rovida, 2002; Hooper et al., 1997). L-selectin also contains two SCRs but in contrast to CD21 it contains a stalk region of about 15 amino acids in between the plasma membrane and SCR2. Point mutations of multiple conserved residues within the identified cleavage site did not inhibit L-selectin shedding but deletions of four to five residues inhibited shedding. The authors concluded that the length of the stalk rather than the sequence is important for L-selectin shedding (Migaki et al., 1995). Based on these findings we suggested that CD21 has to be at least partially reduced to generate a stalk that allows access of the sheddase. A reduction of the disulfide bridge between cys-2 and cys-4 of SCR16 would already generate a juxtamembrane stalk of 14 amino acids in length and a reduction of the disulfide bridge between cys-1 and cys-3 would lead to a stalk of 23 amino acids between SCR16 and SCR15. To test this hypothesis, we developed a system that allowed the exchange of disulfide with diselenide bridges, the latter having a much lower redox potential than disulfide bridges (Besse et al., 1997; Besse and Moroder, 1997; Siedler et al., 1993). The resulting CD21 proteins should therefore be unable to generate such a juxtamembrane stalk upon

stimulation with reducing agents. In case of *E. coli* thioredoxin, a change of two cysteine residues to selenocysteines, forming a disufide bridge in the oxidized protein, led to a stable diselenide bridge, that could not be reduced even in the presence of an excess of 2-ME (Muller et al., 1994). Since selenocysteine (Sec) is encoded by the eukaryotic stop codon UGA, only fully translated CD21-Sec proteins can be incorporated into the plasma membrane and appear at the cell surface. The expression and surface localization of the Sec-containing CD21 proteins was therefore confirmed by immunoprecipitation and flow cytometry. As additional proof, we found that increasing amounts of sodium-selenite in the cell culture medium led to an increase in the cell surface expression of the CD21-Sec proteins. By introduction of a diselenide bridge instead of the cysteine bridge between cys-2 and cys-4 we showed that CD21 shedding is abolished, whereas CD21 proteins, missing this cysteine bridge because of the insertion of methionines, were shed even better than the control proteins. Since there is a strong preference for the formation of a diselenide bridge instead of a hybrid (cys-Sec) bridge (Besse et al., 1997; Besse and Moroder, 1997) it is unlikely that CD21 shedding was inhibited because of structural changes of the CD21-Sec proteins due to the formation of an incorrect cys-Sec bridge. Leonard and co-workers (Leonard et al., 1996) also showed that such a heterologous incorporation of Sec into the rat growth hormone receptor and the human thyroid hormone receptor beta 1 had no negative effect on the expression and signaling activity of the proteins.

Taken together (see Fig. 8), we show that CD21 shedding requires the presence of SCR16. Induction of shedding by PMA/CaI or the oxidizing agent pervanadate involves signaling via PKC and requires a serine protease and a metalloprotease activity. In contrast to this, reducing agents, such as the thiol antioxidants NAC or GSH, depend on the activity of the metallo- but not the serine protease. Furthermore CD21 shedding induced by reducing agents did not, unlike pervanadate, involve tyrosine phosphorylation of proteins or the activity of the PKC. An exchange of the disulfide bridge between cys-2 and cys-4 of SCR16 with a diselenide bridge results in a loss of inducible CD21 shedding, suggesting that changes in the redox-potential result in a reduction of this bridge in order to generate a stalk required to allow access of the sheddase.

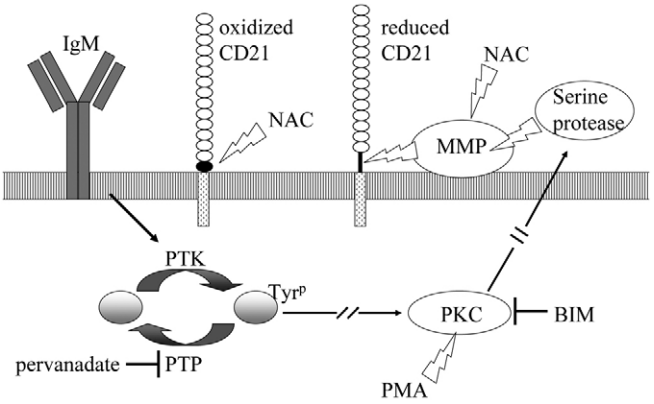

Fig. 8. Schematic representation of proposed mechanisms of CD21 shedding activation. Activation of B cells by BCR and CD40 crosslinking leads to a tyrosine phosphorylation pathway that involves PKC. A similar pathway is activated by pervanadate in B cells, as well as in non-lymphoid cells such as the epithelial cell line 293. Subsequently, a serine protease is activated that is necessary to activate the metalloprotease involved in CD21 shedding. Thiol antioxidants such as NAC directly activate the metalloprotease and open disulfide bridges within the SCRs of CD21. This leads to the formation of a stalk region that permits access of the protease to the cleavage site within SCR16. PMA, phorbol 12-myristate 13-acetate, PTP, protein tyrosine phosphatase; PTK, protein tyrosine kinase; MMP, metalloprotease; TyrP, tyrosine-phosphorylated protein; Bim, bisindolyl maleimid; NAC, N-acetyl cysteine; PKC, protein kinsae C.

Materials and Methods

Chemicals

Phorbol 12-myristate 13-acetate (PMA), ionomycin (CaI), α1-antitrypsin (AAT), reduced L-glutathione (GSH), oxidized L-glutathione (GSSG), N-acetylcysteine (NAC), sodium orthovanadate (Na_3VO_4), β-mercaptoethanol (2-ME), bisindolylmaleimid (BIM), tissue inhibitor of metalloprotease-III (TIMP-III) and sodium selenite were purchased from Sigma-Aldrich (Buchs, Switzerland). Pervanadate was freshly prepared for each experiment by mixing one volume of sodium orthovanadate (100 mM, pH 10) with one volume of H_2O_2 (100 mM) and was used within 10 minutes of preparation. Matrix metalloprotease inhibitor-I, -II, -III (MMPi-I, -II, -III), TIMP-I and -II were purchased from Calbiochem (Lucerne, Switzerland).

Cell culture

The epithelial cell line 293, Daudi B and Raji B cell lines were cultured in Iscove's Modified Dulbecco's Medium (IMDM) supplemented with UltraGlutamine-I (2 mM), penicillin/streptomycin (100 U/ml, 100 μg/ml) (all from Cambrex, Verviers, Belgium) and 10% fetal calf serum (FCS) (Linaris, Wertheim-Bettingen, Germany) (complete IMDM). Cells were maintained at 37°C with 7.5% CO_2. For the incorporation of selenocysteine, cells were cultivated in complete IMDM supplemented with 150 nM sodium selenite.

Construction of CD21 expression plasmids

All cDNAs were cloned into pEGFP-C1 (BD Clontech, Basel, Switzerland) using the *Nhe*I site 5′ to EGFP and sites from the multiple cloning site. Therefore, all constructs were missing the EGFP cDNA from the original plasmid. CD21-encoding sequences were amplified by PCR from the CD21 expression plasmid pSFFVneo-CR2-M1 (Carel et al., 1989) containing the short CD21 cDNA lacking exon 11 (Fujisaku et al., 1989). To obtain a CD21 cDNA lacking exon 16 (Fig. 6 construct A), a two step cloning of exons 1-15 (Tg115: 5′-CATGCGCTAGC-GCCACCATGGGCGCCGCGGGCCTG-3′, containing the EGFP-specific Kozak consensus sequence from plasmid pEGFP-C1 5′ to the translation initiation codon of CD21 and Tg187: 5′-GGAAGATCTTTTACAATGAGGGGCAGGTTGGCTCC-3′), and exons 17-19 (Tg188: 5′-GGAAGATCTCGTTCACTTGCTCCTGTCCT-TTGTGG-3′ + Tg189: 5′-TTGACGTCGACTCAGCTGGCTGGGTTGTATGGAT-CAAC-3′) was performed. Construct B contains the complete CD21 cDNA (Tg115 + Tg189). For construct C, containing a *Bgl*II site 3′ to exon 16, exons 1-16 were amplified (Tg115 + Tg208: 5′-GGAAGATCTGGATCTGCAAACCGCCAGGGG-3′) and inserted into the *Nhe*I/*Bgl*II-digested construct A. Construct D contains a *Bgl*II site 5′ to exon 16. For this, exon 16-19 was amplified (Tg207: 5′-GGAAGATCTGAGGTAAACTGTAGCTCACCAGC-3′ + Tg189) and inserted into the *Bgl*II/*Sal*I digested construct A. Construct E with *Bgl*II sites 5′ and 3′ to exon 16 was obtained by amplification of exon 16 alone (Tg207 + Tg208) and insertion into the *Bgl*II digested construct A. 293 cells stable transfected with these constructs were named 293-CD21-A/-B/-C/-D and -E, respectively. The sequences of all PCR amplified cDNAs were confirmed by sequencing.

Site directed mutagenesis of disulfide bridges within SCR16

Site directed mutagenesis of cysteines cys-2 (Cys941) and cys-4 (Cys968) of CD21 SCR16 was performed using construct E as template for PCR and the QuikChange multi site directed mutagenesis kit (Stratagene, La Jolla CA, USA) following the manufacturer's instructions. For the incorporation of selenocysteines instead of cysteines (construct F), the UGA stop codon of construct CD21-E was changed to UAG using primer Tg215 (5′-TACAACCCAGCCAGCTAGGTCGACGGTACCG-CG-3′). In a second mutagenesis round the cysteine codons of Cys941 and Cys968 were replaced by the selenocysteine codon UGA using primers Tg219 (5′-GCTGTTGTAACTCTGGAGTGAGAAGATGGGTATATGC-3′) for cys-2 and Tg223 (5′-CCTCCCCTGGCGGTTTGAAGATCCAGATCTCG-3′) for cys-4. The selenocysteine-insertion-sequence (SECIS) of the selenium-dependent glutathione peroxidase PHGPx (Muller et al., 2003) was amplified by PCR from 293 cDNA using primers Tg224 (5′-TTGACGTCGACGCTCCACAAGTGTGTGG-3′) and Tg225 (5′-GGTACCGTCGACGTCTGTTTATTCCCACAAGGTA-3′) and inserted via a *Sal*I site 3′ to the UAG stop codon. Cysteines were changed to methionines (construct G) using primers Tg218 (5′-GCTGTTGTAACTCTGGAGATGGAAG-

ATGGGTATATGC-3′) for cys-2 and Tg222 (5′-CCTCCCCTGGCGGTTATGAG-ATCCAGATCTCG-3′) for cys-4. The success of the mutagenesis was verified by sequencing. 293 cells stably transfected with construct F and G were named CD21-Sec and CD21-Met cells, respectively.

Transfection and cloning of 293 cells

5×10^5 293 cells/ml were incubated overnight at 37°C and subsequently transfected with 3 μg plasmid DNA (CD21 constructs A-G or pSFFVneo-CR2-M1) using Metafectene transfection reagent (Biontex, Munich, Germany) according to the manufacturer's instruction. For selection of stable transfected cells, 3 mg/ml G418 (Calbiochem) was added. Cell surface expression of the exogenous proteins was verified by flow cytometry using the anti-CD21 antibody anti-CD21-RPE (clone LB21, Serotec, Oxford, UK). A mixture of stable pSFFVneo-M1-CR2-transfected cells (293-CD21 cells) was used for experiments. Cells expressing one of the constructs A-G were isolated by cell sorting (FACSVantage SE, BD Biosciences, Allschwil, Switzerland) using the antibody anti-CD21-RPE (Serotec) and cloned.

Immunofluorescent staining of 293-CD21 cells

293-CD21 cells were cultured on culture slides (BD Falcon, Basel, Switzerland), fixed with ice-cold methanol for 10 minutes at –20°C and stained using standard protocols with anti-CD21 mAb BL13 (1:100, FITC-labeled) (Immunotech-Beckman Coulter, Nyon, Switzerland). Cell surface CD21 expression was verified by confocal microscopy (LSM 510, Zeiss, Jena, Germany).

Determination of cell surface CD21 by flow cytometry

For analysis of cell surface CD21, 293-CD21 and Daudi cells were stained with anti-CD21-RPE (clone LB21, Serotec, Oxford, UK) and subjected to flow cytometry (BD LSR, BD Biosciences). For analysis of cell surface CD21 on primary B cells, PBMC were gated for B cells after staining with anti-CD21-RPE, anti-CD19-FITC (both Serotec) and anti-CD20-APC (BD Biosciences).

Induction of CD21 shedding

293-CD21 cells were plated at a cell density of 5×10^5 cells/ml and incubated overnight at 37°C. Daudi B cells were adjusted to 2×10^6 cells/ml, Raji B cells to 5×10^6 cells/ml. Cells were incubated in complete IMDM without FCS at 37°C for 2 hours, then fresh medium without FCS was added together with the respective test compounds and cells were incubated for additional 4 hours at 37°C. Peripheral blood mononuclear cells (PBMC) were isolated using BD Vacutainer CPT (BD Biosciences), washed twice in complete IMDM without FCS and subsequently stimulated as described for 293-CD21 and Daudi cells. MMPis, TIMPs or the PKC inhibitor BIM were added to the cell culture 1 or 2 hours before addition of the shedding stimuli, respectively. The viability of the cells upon stimulation did not decrease more than 20% and was determined by TO-PRO-3-iodide staining (500 nM in DMSO) (Molecular Probes, Leiden, Netherlands) and flow cytometry, as well as by Trypane Blue exclusion.

Determination of sCD21 by sandwich ELISA

To determine sCD21 concentrations in cell culture supernatants a CD21 sandwich ELISA using mAb THB5 (2 μg/ml in PBS) for coating and BU32-biotin (0.5 μg/ml in blocking buffer; PBS/3% BSA) for detection, was performed as previously described (Masilamani et al., 2003a). To compare the amounts of sCD21 shedded by different cell types expressing different amounts of CD21, measured sCD21 values were normalized by dividing sCD21 (pg/ml) by the median fluorescence intensity of respective cell types, determined by flow cytometric analysis.

SDS gel electrophoresis and western blotting

At the indicated time points, cells were scraped off the cell culture flasks in ice-cold PBS, collected by centrifugation and lysed for 30 minutes on ice in lysis buffer (1% NP-40, 50 mM NaCl, 50 mM NaF, 30 mM $Na_4P_2O_7$, 5 mM EDTA, 1 mM Na_3VO_4 and 1× complete protease inhibitor cocktail; Roche, Rotkreuz, Switzerland). Proteins were separated using 4-12% Bis/Tris NuPAGE SDS gels (Invitrogen AG, Basel, Switzerland) and blotted onto Protran Nitrocellulose membranes (Schleicher & Schuell GmbH, Dassel, Germany) using standard techniques. Western blotting for CD21 was performed with the monoclonal antibody BU32 using BU32-hybridoma cell culture supernatants. For detection of phosphotyrosines, blots were incubated with anti-pTyr sc-7020 (1:1000) (Santa-Cruz/Lab Force, Nunningen, Switzerland). As loading control, blots were stained with Ponceau Red or incubated with the anti-β-actin antibody ab6276 (1:5000) (Abcam, Cambridge, UK).

Statistical analysis

All experiments were done at least three times. Values in the figures are given as means ± s.e.m. Statistical analysis was performed using GraphPad Instat (Instat Statistics, GraphPad Software, San Diego, USA). For all data, unpaired nonparametric testing with the Mann-Whitney test was performed. The significance is denoted by asterisks: *significant ($P<0.05$), **very significant ($P<0.01$) and ***extremely significant ($P<0.001$).

We thank Eva-Maria Boneberg and Melanie M. Hoefer for critical reading of the manuscript and Elvira Jeisy Walder for technical assistance. This work was supported by the Thurgauische Stiftung für Wissenschaft und Forschung, the Hans-Hench-Stiftung, the EU through grant LSHM-CT-2004-005264 and the Deutsche Stiftung Sklerodermie to H.I.

References

Ahearn, J. M., Fischer, M. B., Croix, D., Goerg, S., Ma, M., Xia, J., Zhou, X., Howard, R. G., Rothstein, T. L. and Carroll, M. C. (1996). Disruption of the Cr2 locus results in a reduction in B-1a cells and in an impaired B cell response to T-dependent antigen. *Immunity* **4**, 251-262.

Althoff, K., Mullberg, J., Aasland, D., Voltz, N., Kallen, K., Grotzinger, J. and Rose-John, S. (2001). Recognition sequences and structural elements contribute to shedding susceptibility of membrane proteins. *Biochem. J.* **353**, 663-672.

Arribas, J. and Merlos-Suárez, A. (2003). Shedding of plasma membrane proteins. In *Current Topics in Developmental Biology: Cell Surface Proteases*. Vol. 54 (ed. S. Zucker and W. T. Chen), pp. 125-144. London: Academic Press.

Arribas, J., Lopez-Casillas, F. and Massague, J. (1997). Role of the juxtamembrane domains of the transforming growth factor-alpha precursor and the beta-amyloid precursor protein in regulated ectodomain shedding. *J. Biol. Chem.* **272**, 17160-17165.

Bacon, K., Gauchat, J. F., Aubry, J. P., Pochon, S., Graber, P., Henchoz, S. and Bonnefoy, J. Y. (1993). CD21 expressed on basophilic cells is involved in histamine release triggered by CD23 and anti-CD21 antibodies. *Eur. J. Immunol.* **23**, 2721-2724.

Besse, D. and Moroder, L. (1997). Synthesis of selenocysteine peptides and their oxidation to diselenide-bridged compounds. *J. Pept. Sci.* **3**, 442-453.

Besse, D., Budisa, N., Karnbrock, W., Minks, C., Musiol, H. J., Pegoraro, S., Siedler, F., Weyher, E. and Moroder, L. (1997). Chalcogen-analogs of amino acids. Their use in x-ray crystallographic and folding studies of peptides and proteins. *Biol. Chem.* **378**, 211-218.

Buhimschi, I. A., Kramer, W. B., Buhimschi, C. S., Thompson, L. P. and Weiner, C. P. (2000). Reduction-oxidation (redox) state regulation of matrix metalloproteinase activity in human fetal membranes. *Am. J. Obstet. Gynecol.* **182**, 458-464.

Carel, J. C., Frazier, B., Ley, T. J. and Holers, M. (1989). Analysis of epitope expression and the functional repertoire of recombinant complement receptor 2 (CR2/CD21) in mouse and human cells. *J. Immunol.* **143**, 923-930.

De Vries, N. and De Flora, S. (1993). N-acetyl-l-cysteine. *J. Cell. Biochem. Suppl.* **17F**, 270-277.

Delibrias, C. C., Mouhoub, A., Fischer, E. and Kazatchkine, M. D. (1994). CR1(CD35) and CR2(CD21) complement C3 receptors are expressed on normal human thymocytes and mediate infection of thymocytes with opsonized human immunodeficiency virus. *Eur. J. Immunol.* **24**, 2784-2788.

Dello Sbarba, P. and Rovida, E. (2002). Transmodulation of cell surface regulatory molecules via ectodomain shedding. *Biol. Chem.* **383**, 69-83.

Fingeroth, J. D., Weis, J. J., Tedder, T. F., Strominger, J. L., Biro, P. A. and Fearon, D. T. (1984). Epstein-Barr virus receptor of human B lymphocytes is the C3d receptor CR2. *Proc. Natl. Acad. Sci. USA* **81**, 4510-4514.

Fingeroth, J. D., Diamond, M. E., Sage, D. S., Hayman, J. and Yates, J. L. (1999). CD21-dependent infection of an epithelial cell line, 293, by Epstein-Barr virus. *J. Virol.* **73**, 2115-2125.

Fischer, E., Delibrias, C. and Kazatchkine, M. D. (1991). Expression of CR2 (the C3dg/EBV receptor, CD21) on normal human peripheral blood T lymphocytes. *J. Immunol.* **146**, 865-869.

Fischer, M. B., Goerg, S., Shen, L., Prodeus, A. P., Goodnow, C. C., Kelsoe, G. and Carroll, M. C. (1998). Dependence of germinal center B cells on expression of CD21/CD35 for survival. *Science* **280**, 582-585.

Fremeaux-Bacchi, V., Aubry, J. P., Bonnefoy, J. Y., Kazatchkine, M. D., Kolb, J. P. and Fischer, E. M. (1998). Soluble CD21 induces activation and differentiation of human monocytes through binding to membrane CD23. *Eur. J. Immunol.* **28**, 4268-4274.

Fujisaku, A., Harley, J. B., Frank, M. B., Gruner, B. A., Frazier, B. and Holers, V. M. (1989). Genomic organization and polymorphisms of the human C3d/Epstein-Barr virus receptor. *J. Biol. Chem.* **264**, 2118-2125.

Gasque, P., Chan, P., Mauger, C., Schouft, M. T., Singhrao, S., Dierich, M. P., Morgan, B. P. and Fontaine, M. (1996). Identification and characterization of complement C3 receptors on human astrocytes. *J. Immunol.* **156**, 2247-2255.

Hooper, N. M., Karran, E. H. and Turner, A. J. (1997). Membrane protein secretases. *Biochem. J.* **321**, 265-279.

Huemer, H. P., Larcher, C., Prodinger, W. M., Petzer, A. L., Mitterer, M. and Falser, N. (1993). Determination of soluble CD21 as a parameter of B cell activation. *Clin. Exp. Immunol.* **93**, 195-199.

Janatova, J., Reid, K. B. and Willis, A. C. (1989). Disulfide bonds are localized within the short consensus repeat units of complement regulatory proteins: C4b-binding protein. *Biochemistry* **28**, 4754-4761.

Kaup, M., Dassler, K., Weise, C. and Fuchs, H. (2002). Shedding of the transferrin receptor is mediated constitutively by an integral membrane metalloprotease sensitive to tumor necrosis factor alpha protease inhibitor-2. *J. Biol. Chem.* **277**, 38494-38502.

Krol, A. (2002). Evolutionarily different RNA motifs and RNA-protein complexes to achieve selenoprotein synthesis. *Biochimie* **84**, 765-774.

Le Gall, S. M., Auger, R., Dreux, C. and Mauduit, P. (2003). Regulated cell surface

pro-EGF ectodomain shedding is a zinc metalloprotease-dependent process. *J. Biol. Chem.* **278**, 45255-45268.

Leonard, J. L., Leonard, D. M., Shen, Q., Farwell, A. P. and Newburger, P. E. (1996). Selenium-regulated translation control of heterologous gene expression: normal function of selenocysteine-substituted gene products. *J. Cell Biochem.* **61**, 410-419.

Ling, N., Hansel, T., Richardson, P. and Brown, B. (1991). Cellular origins of serum complement receptor type 2 in normal individuals and in hypogammaglobulinaemia. *Clin. Exp. Immunol.* **84**, 16-22.

Lowe, J., Brown, B., Hardie, D., Richardson, P. and Ling, N. (1989). Soluble forms of CD21 and CD23 antigens in the serum in B cell chronic lymphocytic leukaemia. *Immunol. Lett.* **20**, 103-109.

Masilamani, M., Apell, H. J. and Illges, H. (2002). Purification and characterization of soluble CD21 from human plasma by affinity chromatography and density gradient centrifugation. *J. Immunol. Methods* **270**, 11-18.

Masilamani, M., Kassahn, D., Mikkat, S., Glocker, M. O. and Illges, H. (2003a). B cell activation leads to shedding of complement receptor type II (CR2/CD21). *Eur. J. Immunol.* **33**, 2391-2397.

Masilamani, M., von Kempis, J. and Illges, H. (2003b). Decreased levels of serum soluble complement receptor-II (CR2/CD21) in patients with rheumatoid arthritis. *Rheumatology Oxford* **43**, 186-190.

Masilamani, M., Nowack, R., Witte, T., Schlesier, M., Warnatz, K., Glocker, M. O., Peter, H. H. and Illges, H. (2004). Reduction of soluble complement receptor II/CD21 in systemic lupus erythomatosus and Sjoegren's syndrome but not juvenile arthritis. *Scand. J. Immunol.* **60**, 625-630.

Migaki, G. I., Kahn, J. and Kishimoto, T. K. (1995). Mutational analysis of the membrane-proximal cleavage site of L-selectin: relaxed sequence specificity surrounding the cleavage site. *J. Exp. Med.* **182**, 549-557.

Moore, M. D., Cooper, N. R., Tack, B. F. and Nemerow, G. R. (1987). Molecular cloning of the cDNA encoding the Epstein-Barr virus/C3d receptor (complement receptor type 2) of human B lymphocytes. *Proc. Natl. Acad. Sci. USA* **84**, 9194-9198.

Muller, C., Wingler, K. and Brigelius-Flohe, R. (2003). 3′UTRs of glutathione peroxidases differentially affect selenium-dependent mRNA stability and selenocysteine incorporation efficiency. *Biol. Chem.* **384**, 11-18.

Muller, S., Senn, H., Gsell, B., Vetter, W., Baron, C. and Bock, A. (1994). The formation of diselenide bridges in proteins by incorporation of selenocysteine residues: biosynthesis and characterization of (Se)2-thioredoxin. *Biochemistry* **33**, 3404-3412.

Myones, B. L. and Ross, G. D. (1987). Identification of a spontaneously shed fragment of B cell complement receptor type two (CR2) containing the C3d-binding site. *Complement* **4**, 87-98.

Nishinaka, Y., Nakamura, H., Okada, N., Okada, H. and Yodoi, J. (2001). Redox control of EBV infection: prevention by thiol-dependent modulation of functional CD21/EBV receptor expression. *Antioxid. Redox Signal.* **3**, 1075-1087.

Perkins, S. J., Gilbert, H. E., Aslam, M., Hannan, J., Holers, V. M. and Goodship, T. H. (2002). Solution structures of complement components by x-ray and neutron scattering and analytical ultracentrifugation. *Biochem. Soc. Trans.* **30**, 996-1001.

Qin, D., Wu, J., Carroll, M. C., Burton, G. F., Szakal, A. K. and Tew, J. G. (1998). Evidence for an important interaction between a complement-derived CD21 ligand on follicular dendritic cells and CD21 on B cells in the initiation of IgG responses. *J. Immunol.* **161**, 4549-4554.

Reth, M. (2002). Hydrogen peroxide as second messenger in lymphocyte activation. *Nat. Immunol.* **3**, 1129-1134.

Reynes, M., Aubert, J. P., Cohen, J. H., Audouin, J., Tricottet, V., Diebold, J. and Kazatchkine, M. D. (1985). Human follicular dendritic cells express CR1, CR2, and CR3 complement receptor antigens. *J. Immunol.* **135**, 2687-2694.

Schieven, G. L., Kirihara, J. M., Myers, D. E., Ledbetter, J. A. and Uckun, F. M. (1993). Reactive oxygen intermediates activate NF-kB in a tyrosine kinase-dependent mechanism and in combination with vanadate activate the $p56^{lck}$ and $p59^{fyn}$ tyrosine kinases in human lymphocytes. *Blood* **82**, 1212-1220.

Schwab, J. and Illges, H. (2001). Regulation of CD21 expression by DNA methylation and histone deacetylation. *Int. Immunol.* **13**, 705-710.

Siedler, F., Rudolph-Bohner, S., Doi, M., Musiol, H. J. and Moroder, L. (1993). Redox potentials of active-site bis(cysteinyl) fragments of thiol-protein oxidoreductases. *Biochemistry* **32**, 7488-7495.

Steiner, D. F., Smeekens, S. P., Ohagi, S. and Chan, S. J. (1992). The new enzymology of precursor processing endoproteases. *J. Biol. Chem.* **267**, 23435-23438.

Tedder, T. F., Clement, L. T. and Cooper, M. D. (1984). Expression of C3d receptors during human B cell differentiation: immunofluorescence analysis with the HB-5 monoclonal antibody. *J. Immunol.* **133**, 678-683.

Uckun, F. M., Tuel-Ahlgren, L., Song, C. W., Waddick, K., Myers, D. E., Kirihara, J., Ledbetter, J. A. and Schieven, G. L. (1992). Ionizing radiation stimulates unidentified tyrosine-specific protein kinases in human B-lymphocyte precursors, triggering apoptosis and clonogenic cell death. *Proc. Natl. Acad. Sci. USA* **89**, 9005-9009.

Uemura, S., Matsushita, H., Li, W., Glassford, A. J., Asagami, T., Lee, K. H., Harrison, D. G. and Tsao, P. S. (2001). Diabetes mellitus enhances vascular matrix metalloproteinase activity: role of oxidative stress. *Circ. Res.* **88**, 1291-1298.

Van Wart, H. E. and Birkedal-Hansen, H. (1990). The cysteine switch: A principle of regulation of metalloproteinase activity with potential applicability to the entire matrix metalloproteinase gene family. *Proc. Natl. Acad. Sci. USA* **87**, 5578-5582.

Velasco-Loyden, G., Arribas, J. and Lopez-Casillas, F. (2004). The shedding of betaglycan is regulated by pervanadate and mediated by membrane type matrix metalloprotease-1. *J. Biol. Chem.* **279**, 7721-7733.

Weis, J. J., Tedder, T. F. and Fearon, D. T. (1984). Identification of a 145,000 Mr membrane protein as the C3d receptor (CR2) of human B lymphocytes. *Proc. Natl. Acad. Sci. USA* **81**, 881-885.

Weis, J. J., Toothaker, L. E., Smith, J. A., Weis, J. H. and Fearon, D. T. (1988). Structure of the human B lymphocyte receptor for C3d and the Epstein-Barr virus and relatedness to other members of the family of C3/C4 binding proteins. *J. Exp. Med.* **168**, 1953-1954.

Zucker, S., Pei, D., Cao, J. and Lopez-Otin, C. (2003). Membrane type-matrix metalloproteinases (MT-MMP). In *Current Topics in Developmental Biology: Cell Surface Proteases.* Vol. 54 (ed. S. Zucker and W. T. Chen), pp. 1-74. London: Academic Press.